Individualized Biventricular Epicardial Augmentation Technology in a Drug-Induced Porcine Failing Heart Model

Lasse Jagschies,* Marc Hirschvogel,* Jose Matallo,† Andreas Maier,‡ Karin Mild,§ Horst Brunner,§ Rabea Hinkel,¶ ‖ # Michael W. Gee,* Peter Radermacher,† Stephen M. Wildhirt,‡ and Sebastian Hafner†**

For treatment of advanced heart failure, current strategies include cardiac transplantation or blood-contacting pump technology associated with complications, including stroke and bleeding. This study investigated an individualized biventricular epicardial augmentation technology in a drug-induced porcine failing heart model. A total of 11 pigs were used, for the assessment of hemodynamics and cardiac function under various conditions of support pressures and support durations (n = 4), to assess device positioning and function by *in vivo* computer tomographic imaging (n = 3) and to investigate a minimally invasive implantation on the beating heart (n = 4). Support pressures of 20–80 mm Hg gradually augmented cardiac function parameters in this animal model as indicated by increased left ventricular stroke volume, end-systolic pressures, and decreased end-diastolic pressures. Strong evidence was found regarding the necessity of mechanical synchronization of support end with the isovolumetric relaxation phase of the heart. In addition, the customized, self-expandable implant enabled a marker-guided minimally invasive implantation through a 4 cm skin incision using fluoroscopy. Correct positioning was confirmed in computer tomographic images. Continued long-term survival investigations will deliver preclinical evidence for further development of this concept. *ASAIO Journal* 2018; 64:480–488.

Key Words: biventricular assist device, heart failure, extravascular, minimally invasive implantation

To date, many attempts have been made to improve the outcome of patients with implanted ventricular assist devices (VADs) in order to establish a true alternative to heart transplantation. Pruijsten *et al*. reported an extensive hemodynamic recovery compatible with daily life activities in left ventricular (LV) assist device (LVAD) patients. They suggested that improved survival with newer generation devices will provide an alternative to heart transplantation in selected patients.[1] Current VAD technology is associated with a high rate of complications, rehospitalization, and cost.[2] Even though improvements have been made regarding adverse event rate and survival, a high rate of patients experience at least one major complication within 12 months after implantation.[3,4]

Recent efforts focus on the development of less complex, minimally invasive strategies for mechanical cardiac support. One key strategy is to avoid blood contact as the major driver for complications such as stroke and bleeding. Some extravascular devices were intended to compressing the ventricles of the heart using pneumatic or hydraulic expandable units positioned inside the pericardial space.[5–8] These devices were mainly investigated in the scope of acute heart failure (HF) animal models. However, promising results have clearly shown the potential of this technology in five human patients with cardiogenic shock.[9] It may also serve as an adjunctive, less complex therapeutic approach to established blood-contacting impeller pumps that are currently used to treat advanced HF patients.

In the current study, we investigated a novel biventricular epicardial augmentation technology (AdjuCor GmbH, Munich, Germany) in an acute, drug-induced porcine failing heart model. The technology specifically addresses requirements for potential clinical use: 1) customized, patient-specific configuration of the implant to allow unconstrained diastolic relaxation and filling; 2) reliable and exact synchronization to each cardiac cycle as a mandatory prerequisite for the augmentation of cardiac hemodynamics; 3) uni- and biventricular support with adjustable subsystemic pressure ranges for gradual augmentation of impaired cardiac function parameters; and 4) self-expandable material for a minimally invasive implantation on the beating heart.

Methods

The investigation conforms to the "Guide for the Care and Use of Laboratory Animals" published by the US National

From the *Mechanics and High Performance Computing Group, Technical University of Munich, Garching, Germany; †Institut für Anästhesiologische Pathophysiologie und Verfahrensentwicklung, Universitätsklinikum Ulm, Ulm, Germany; ‡AdjuCor GmbH, Garching, Germany; §Klinik für Diagnostische und Interventionelle Radiologie, Universitätsklinikum Ulm, Ulm, Germany; ¶Institute for Cardiovascular Prevention (IPEK), LMU, Munich, Germany; ‖I. Medizinische Klinik, Klinikum Rechts der Isar, TUM, Munich, Germany; #DZHK (German Center for Cardiovascular Research), partner site Munich Heart Alliance, Munich, Germany; and **Klinik für Anästhesiologie, Universitätsklinikum Ulm, Ulm, Germany.

Submitted for consideration March 2017; accepted for publication in revised form August 2017.

This work was supported by the Bavarian Research Foundation (AZ 1020-12, AZ 1114-14); the Federal Ministry for Economic Affairs and Energy of Germany (KF3349001CR); and the 7th framework program of the European Union (AMCARE).

Dr. Andreas Maier serves as CTO and Dr. Stephen Wildhirt serves as CEO for AdjuCor GmbH. AdjuCor GmbH holds patents for the technology described. Prof. Radermacher received grants from AdjuCor GmbH during the conduct of the study. The rest of the authors have nothing to disclose.

Supplemental digital content is available for this article. Direct URL citations appear in the printed text, and links to the digital files are provided in the HTML and PDF versions of this article on the journal's Web site (www.asaiojournal.com).

Correspondence: Sebastian Hafner, Institut für Anästhesiologische Pathophysiologie und Verfahrensentwicklung, Universitätsklinikum Ulm, Helmholtzstrasse 8-1, 89081 Ulm, Germany. Email: sebastian.hafner@gmx.de.

Copyright © 2017 by the ASAIO

DOI: 10.1097/MAT.0000000000000686

Copyright © American Society of Artificial Internal Organs. Unauthorized reproduction of this article is prohibited.

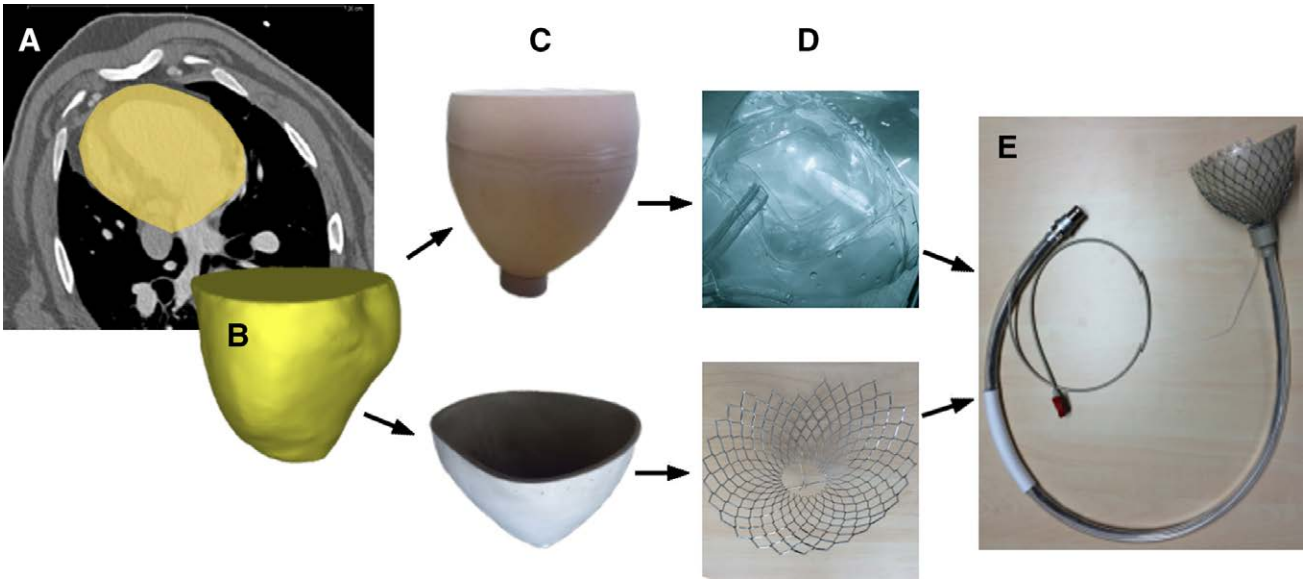

Figure 1. Patient-specific device manufacture: after segmentation of computer tomography (CT) data (**A**), three-dimensional (3D) surface rendering technique is used to create virtual 3D geometries (**B**). This is followed by the production of patient-specific implant forms (**C**), which serve as molds for the implant's components (**D**). These are assembled and connected to the pneumatic tubes (**E**). full color online

Institutes of Health (NIH Publication No. 85-23, revised 1985). The experimental protocol was approved by the institutional "Animal Care and Use Committee" of the University of Ulm, Germany, and the legal authority of the State of Baden-Württemberg, Germany, and the institutional "Animal Care and Use Committee" of the State of Bavaria, Munich, Germany.

Eleven pigs of either gender with a median (interquartile range) body weight of 83 (70–86) kg were used to study device function *in vivo*: Four pigs were used for catheter-based assessment of cardiac function parameters. Three pigs were used for computer tomographic (CT) imaging of anatomic fit and device function. Four pigs were used for evaluation of a closed-chest interventional device implantation. After the experiments, animals were sacrificed under deep anaesthesia.

Individualized Implant Development, Design, and Production

The implant manufacturing process is based on a CT scan of each individual pig heart before the experiment day. It was triggered to the time point of maximum diastolic filling. The CT images were used to segment the ventricular portion of the heart from the apex to the valve plane using MIMICS software (Materialise, Leuven, Belgium; **Figure 1A**). Based on the resulting virtual and real three-dimensional (3D) models of the pig's heart (**Figure 1, B and C**), an offset nitinol sheath and a fitting polyurethane sleeve resembling the shape of the ventricles were manufactured (**Figure 1D**) and bonded (**Figure 1E**). Three inflatable pneumatic units were positioned to the inside of the implant according to anatomically predefined locations of each individual animal, two facing opposite sides of the LV and one facing the right ventricle (RV). They were tested to withstand millions of inflation cycles within the given pressure range of 20–80 mm Hg.

Electropneumatic Control Unit

The electrocardiogram (ECG) was used as a physiological input signal for the pneumatic control unit. It was sensed through an endocardially placed electrode, connected to an integrated electronic control circuit in the driving unit. During support, all pneumatic units were inflated immediately after R-wave detection by opening electronically controlled solenoid valves. The valves were regulated by a proportional integral differential controller for precise support pressure control. The necessary supply pressure was created by a brushless motor in a closed pressure reservoir and transmitted by three different tubes, leading to the pneumatic support units on the epicardium. Controlled active deflation of the support units during diastole was achieved by connecting the supply tubes to a closed low-pressure reservoir. This was done by opening three separate solenoid valves.

Support started during the isovolumetric contraction phase of the heart (**Figure 2**). Support duration t_{SD} was adjusted for variations in heart rate (HR) in each cardiac cycle *via* a linear approximation of Bazett's and Fridericia's formula[10]:

$$t_{SD} = -2\ \text{ms/bpm} \cdot \text{HR} + t_{offset} \quad (1)$$

t_{offset} was taken from the ECG and LV–pressure curves individually for each pig such that the pneumatic units were deflated during isovolumetric relaxation phase (**Figure 2**). To assess the effects of support duration on cardiac function parameters, t_{SD} was varied between 80% and 110% of the actual systolic length T_{sys} during a subset of measurements.

Anaesthesia and Open-Chest Implantation

After premedication, anaesthesia was induced with propofol (1–2 mg/kg) and S-ketamine (0.5–1.0 mg/kg). After endotracheal intubation, anaesthesia, analgesia, and muscle relaxation were achieved with continuous pentobarbitone (8 mg/[kg h]), pancuronium (0.1 mg/[kg·h]), and intermittent buprenorphine (20–30 µg/kg) before painful stimuli. A central-venous catheter, an arterial catheter, a fast response pulmonary artery catheter (CCOmbo; Edwards Lifesciences, Irvine, CA) and a LV pressure–conductance (PV) catheter were placed via the neck

Copyright © American Society of Artificial Internal Organs. Unauthorized reproduction of this article is prohibited.

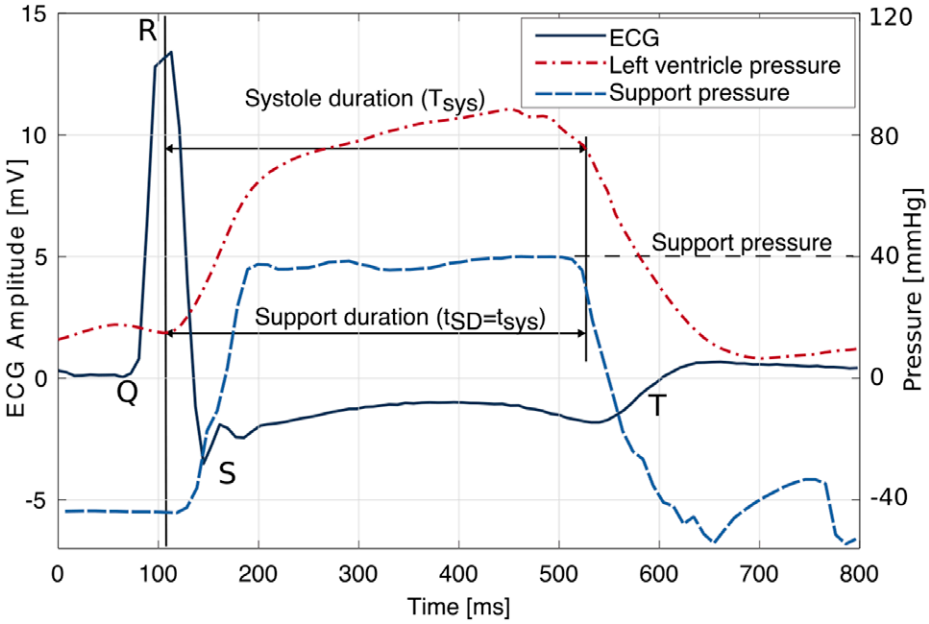

Figure 2. The QRS complex of the electrocardiogram (ECG) is used as the trigger for support synchronization to each cardiac cycle by the electropneumatic driver. Individual support pressures for left and right ventricle as well as support duration may be freely adjusted. An example of support pressure of 40 mm Hg with its duration equal to the systolic length is shown. full color online

vessels for drug infusions, blood sampling, and continuous measurement of mean arterial pressure, mixed-venous hemoglobin oxygen saturation, RV end-diastolic volume, ejection fraction (EF), and LV end-systolic and end-diastolic pressures (LVESP and LVEDP). A transpulmonary thermodilution catheter (PiCCO) was placed via the femoral artery to continuously measure cardiac output (CO) and stroke volume (SV).

For the functional assessments, implantation was performed *via* a lower partial sternotomy and partial pericardiotomy (**Figure 3, A and B**). The customized implants were positioned on the beating heart *via* the apex respecting the animals' anatomy such that the pneumatic units were positioned according to the predefined locations (**Figure 3C**). Customization of the implants significantly facilitated the implantation by

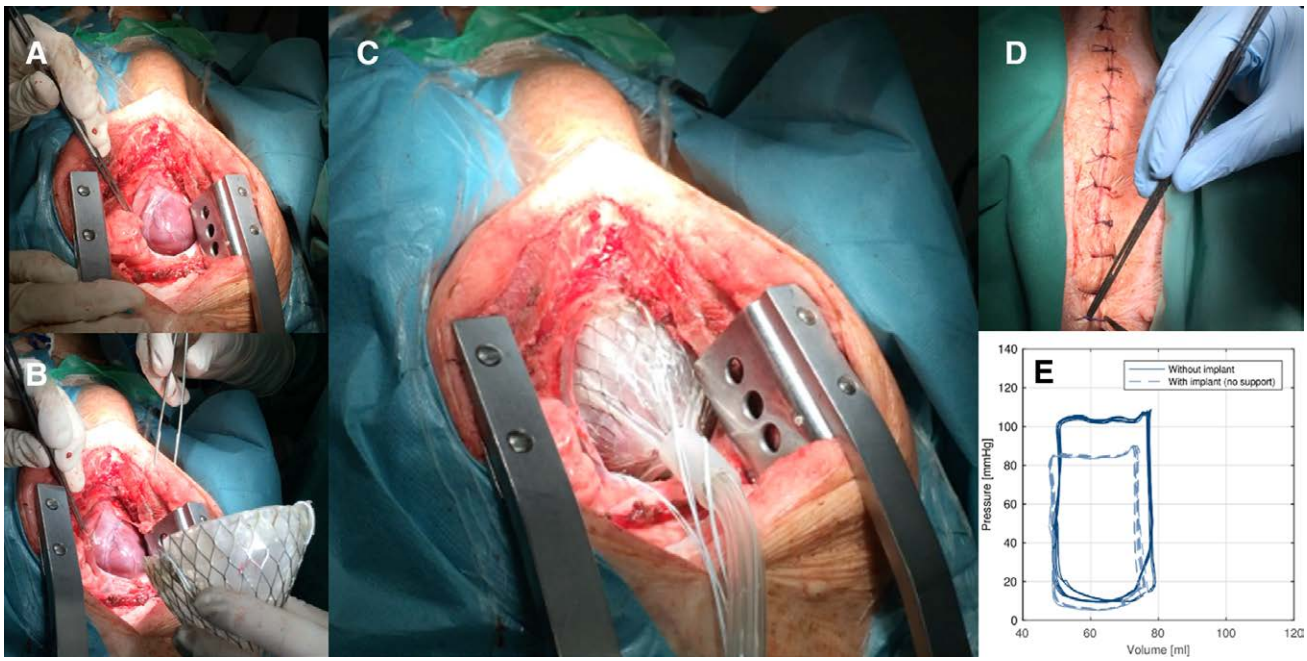

Figure 3. Implantation and positioning: stable device positioning was achieved after lower partial sternotomy and pericardiotomy (**A**). Correct anterior-posterior orientation of the device was mandatory to achieve unrestricted filling of the heart during diastole (**B** and **C**). The chest was closed for all functional experiments (**D**). Pressure–volume (PV) loops before and after device implantation showed no signs for left ventricular restriction by the device (**E**). full color online

Copyright © American Society of Artificial Internal Organs. Unauthorized reproduction of this article is prohibited.

self-positioning/orientation during the first few beats. The chest remained closed throughout the measurements (**Figure 3D**)

Catheter-Based Measurements (n = 4)

Normal cardiac function was assessed with and without the implant to account for restrictions of diastolic relaxation and filling. The heart in normal state was not actuated. The hemodynamic state of an acute HF was then induced by β_1-blockade with 1 mg/kg bolus esmolol followed by a continuous infusion at 170 µg/(kg·min) and doubling of the pentobarbitone dose. Once hemodynamic parameters were stable, changes of cardiac function parameters from baseline values were assessed with respect to LV and RV support pressures and variations in support duration (**Figure 2**). Data were always collected for 30 s, 5 to 10 min after the start of epicardial support.

In Vivo *Device Imaging (n = 3)*

In three animals, anatomic fit and positioning of the implant and visualization of biventricular assist device (BiVAD), LVAD, and RV assist device (RVAD) support were assessed. Furthermore, LV stroke volume (LVSV) changes and EF of the LV and RV were measured by a team of two radiologists and two experienced professionals who performed CT volumetry using Simpson's method.

Afterwards, asystole was induced in pentobarbitone anaesthesia with potassium chloride to study a fixed-frequency BiVAD support mode for the duration of 30 min.

Closed-Chest Implantation (n = 4)

Using four animals, we developed a closed-chest implantation technique. Through a 4–5 cm median subxyphoideal skin incision, the pericardium was opened. The self-expandable implants were radially crimped down to 30 mm (**Figure 4A**) in cold saline and inserted into the chest (**Figure 4B**). A safe and straightforward expansion of the implant into the pericardial space was achieved under fluoroscopic control (**Figure 4, D–F**). Care was taken to respect the anterior–posterior orientation. We observed a final self-alignment in circumferential direction. Correct positioning was confirmed within the intact pericardium after partial sternotomy (**Figure 4G**).

Statistical Evaluation

Data are presented as median (interquartile range) unless otherwise stated. Hemodynamic changes during support were assessed using a linear fixed-effects model.[11] This regression-based statistical model was preferred more than traditional statistical tests such as analysis of variance as it is more robust when dealing with missing measurements and a lack in precision of the control variables. The following equation was fitted to the data set to analyze whether LV support pressure P_{LV}, RV support pressure P_{RV}, and support duration D, respectively, had a significant influence on cardiac function parameter changes:

$$Y = c_1 \times P_{LV} + c_2 \times P_{RV} + c_3 \times D + e \quad (2)$$

with Y being LVSV, LVESP, or LVEDP, respectively, and e the remaining error term.

The coefficient estimates c_j, $j = 1,2,3$ were calculated from a multiple regression analysis through the origin, using a maximum pseudo likelihood fit of the model to the data set. Their value is the slope of the linear dependency between control variable and cardiac function parameter. They were tested for statistically significant difference from 0—corresponding to "no dependence on this variable"—using t-statistic tests. The residuals were analyzed for normal distribution with mean equal to zero to ensure that the data was well described by the model.

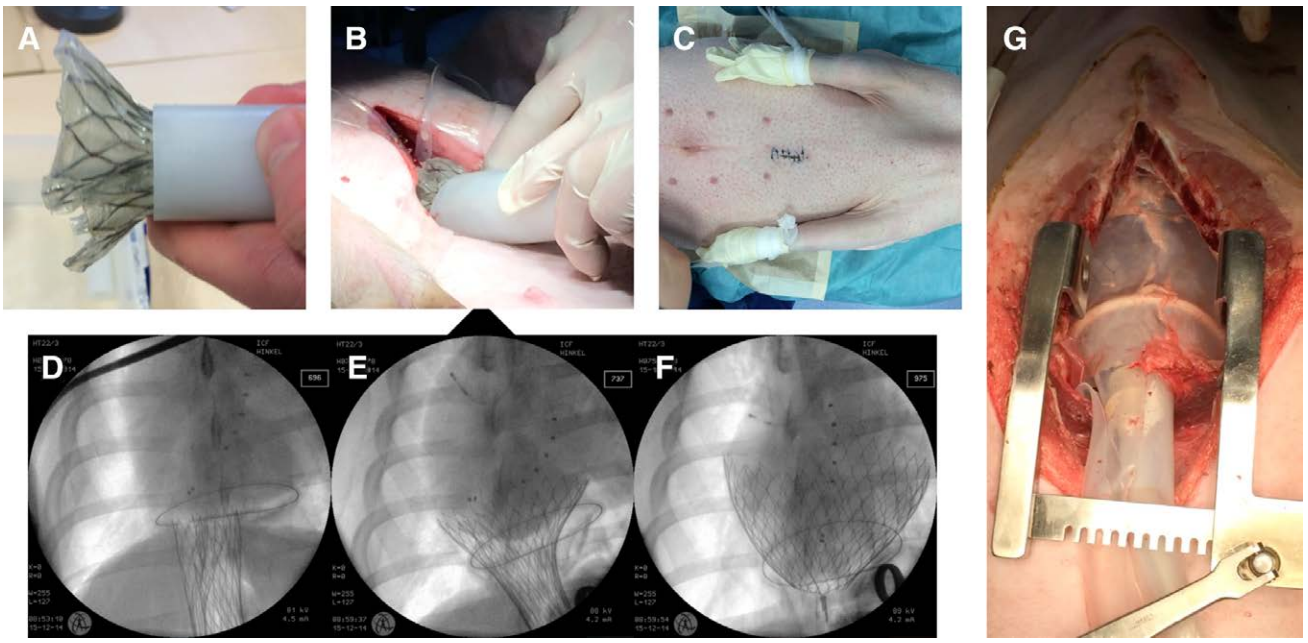

Figure 4. Closed chest minimally invasive device implantation. The implant was crimped to a diameter of 30 mm after cooling (**A**). The crimped implant was brought through the opened pericardium via a small sub-xyphoideal incision (median axis of the heart in pigs; **B**) before skin closure (**C**). Thereafter, circumferential expansion while the implant was ascending around the beating heart was controlled via fluoroscopy (**D–F**). Inspection of the in situ device position with sternotomy and intact pericardium (**G**). full color online

Copyright © American Society of Artificial Internal Organs. Unauthorized reproduction of this article is prohibited.

Table 1. Hemodynamic Parameters Before and After Device Implantation as well as After Induction of Heart Failure

	Normal Heart Without Implant	Normal Heart With Implant	Heart Failure
SV (ml) (PAC)	67 (59–79)	72 (65–76)	54 (43–59)
EF (%) (PAC)	41 (39–45)	40 (37–50)	27 (17–37)
HR (bpm)	103 (92–110)*	78 (74–94)	63 (62–80)
MAP (mm Hg)	100 (87–116)	92 (77–103)	61 (50–68)
SvO_2 (%) (BGA)	77 (72–81)	74 (65–77)	56 (48–62)
EDV (ml) (PAC)	163 (145–192)	170 (143–204)	198 (160–278)

Data are presented as median (interquartile range). Differences of Normal heart with implant to Normal heart without implant were analyzed using a paired *t* test. Presented SV, EF, and EDV values are right ventricular.

**p* value lower than 0.05 *versus* Normal heart without implant.

BGA, mixed venous blood gas analysis; EDV, end-diastolic volume; EF, ejection fraction; HR, heart rate; MAP, mean arterial pressure; PAC, pulmonary artery catheter; SV, stroke volume; SvO_2, mixed venous oxygen saturation.

Results

In all 11 animals, customized implants were successfully positioned around the heart through a partial lower sternotomy or subxyphoideal closed-chest approach. In most animals, we observed some manipulation-induced arrhythmias during implantation without hemodynamic instability. However, after implantation, all animals were found in stable sinus rhythm (**Table 1**).

Catheter-Based Measurements

Figure 3E shows changes in a representative PV loop, observed after device implantation and reduction in HR. Unrestricted LV function, especially end-diastolic filling, was preserved. In addition, CT images revealed no signs of compromised ventricular filling (**Figure 7A**).

Changes of cardiac function parameters with respect to support duration t_{SD} and support pressures P_{LV} and P_{RV} in the functional HF state are shown in **Figures 5 and 6**. **Figure 5A** shows an early stop of support (arrow at 90% systole length) during systole, which causes an immediate drop in LV pressure. In **Figure 5B**, support duration was set to the length of the systole (100%), resulting in an undisturbed morphology of the ventricular pressure curve. Prolonging the support duration towards the early diastolic filling phase (110%) as shown in **Figure 5C** leads to an extended isovolumetric relaxation period.

Changes in LVEDP, LVESP, and LVSV during BiVAD, LVAD, and isolated RV (RVAD) support for different support pressures are shown in **Figure 6A**. All values were calculated as differences to their individual baseline without support. All support modes elevated LVESP and LVSV proportional to the increasing support pressure. However, although BiVAD and LVAD support decreased LVEDP, it was increased during RVAD support. The LV pressure curves during BiVAD support are shown in **Figure 6B**.

Figure 6C summarizes the results of the statistical analysis of the complete data set. Statistically significant dependencies with $p < 0.05$ were found with increasing LV or RV support pressures and when prolonging support duration from 80% systole duration to 100% systole duration as indicated by the arrows. Arrows pointing up indicate proportional behavior and arrows pointing down indicate antiproportional behavior of the cardiac function parameter with respect to the control variable

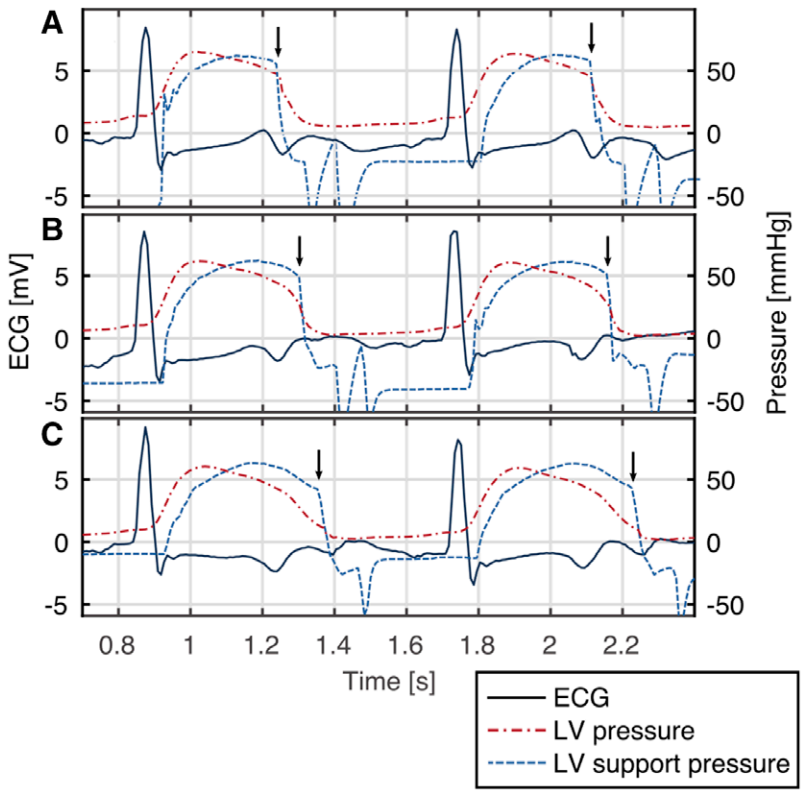

Figure 5. Variation of support duration in a stepwise manner to provide optimized cardiac augmentation within the individual electromechanical window; support end at 90% (**A**), 100% (**B**), and 110% (**C**) systole duration is indicated by the arrow and results in an immediate drop of left ventricular (LV) pressure. ECG, electrocardiogram. full color online

Copyright © American Society of Artificial Internal Organs. Unauthorized reproduction of this article is prohibited.

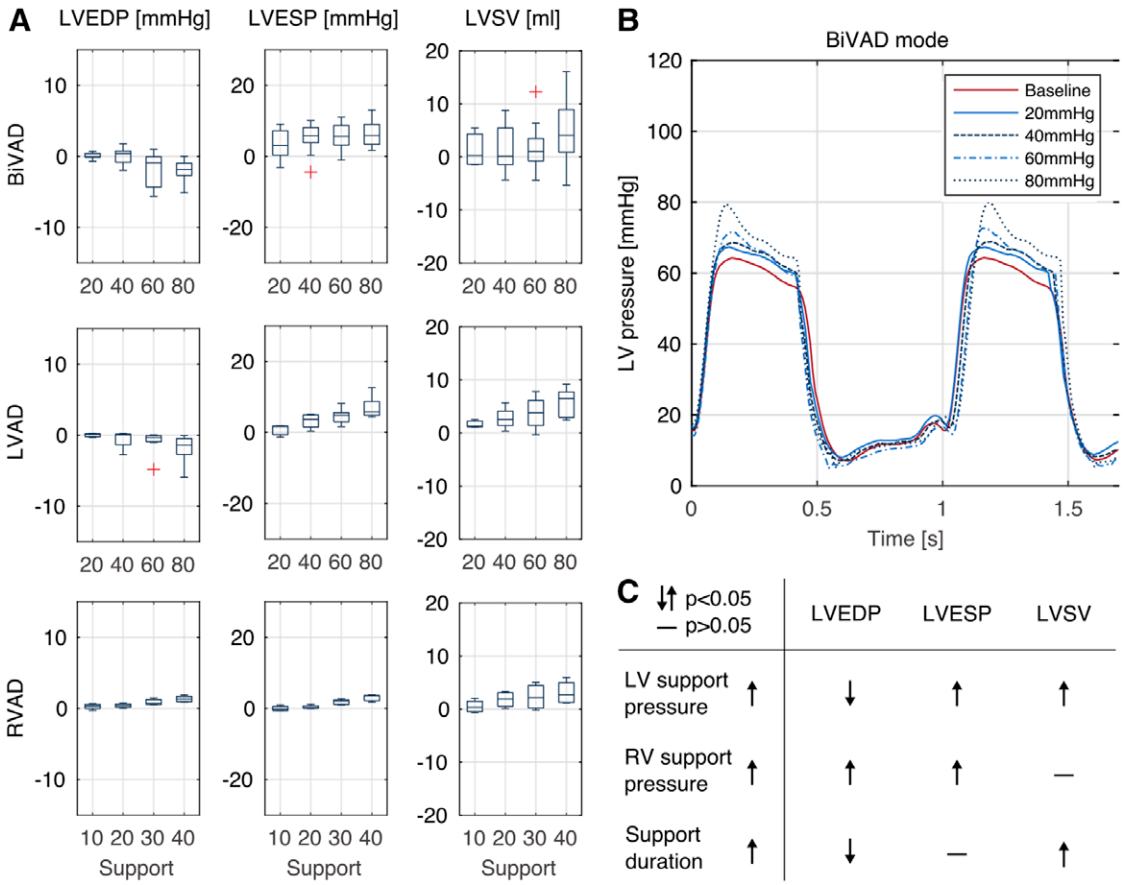

Figure 6. A: Hemodynamic changes from baseline are shown for biventricular assist device (BiVAD), left ventricular assist device (LVAD), and right ventricular assist device (RVAD) support in the functional heart failure cardiac state. Boxplots show median, interquartile range, and min/max values of left ventricular (LV) end-diastolic pressure (LVEDP), end-systolic pressure (LVESP), and stroke volume (LVSV). **B**: Pressure curves for baseline and during biventricular support (LV unit pressure in mm Hg as indicated, RV unit pressure is 20 mm Hg in all cases). **C**: Results of the statistical analysis: Arrows indicate significant proportional or antiproportional dependency of the respective cardiac function parameter on the control variables. full color online

(see Table, Supplemental Digital Content, http://links.lww.com/ASAIO/A187). Statistical significance was not reached for the dependency of LVESP on support duration and for the dependency of LVSV on RV support pressure, although the bottom right graph of **Figure 6A** might suggest otherwise.

In Vivo *Device Imaging*

The effects of BiVAD, LVAD and RVAD support are shown for the end-systolic and end-diastolic phase in **Figure 7A** and supplemental video 1 (see Video, Supplemental Digital Content, http://links.lww.com/ASAIO/A185). *In vivo* imaging also confirmed the importance for individualizing implant design in order to respect their fit and their positioning according to the major blood vessels. **Figure 7B** shows close proximity of the upper rim of the implant to the pulmonary veins and the inferior vena cava, both of which might otherwise be easily compromised by implant.

Changes in LVSV by means of CT volumetry during BiVAD support were 4.1 (4.0–4.3) ml for P_{LV} = 40 mm Hg and 5.7 (4.9–6.5) ml for P_{LV} = 60 mm Hg and lie within the interquartile range of the PiCCO-based measurements shown in **Figure 6A**. EF of the RV and LV in both BiVAD and LVAD mode showed an increase, indicating biventricular support (**Figure 7C**). RVAD support did not have significant effects on EF.

BiVAD Support During Cardiac Arrest

We performed 30 min of BiVAD support at 120 bpm with LV support pressure of 100 mm Hg and RV support pressure of 20 mm Hg after induction of asystole by potassium chloride and pentobarbitone overdose. The device was able to maintain a CO of 2.5 (2.4–2.8) L/min at a mean arterial pressure of 35 (34–36) mm Hg (**Figure 8A**). In some animals, spontaneous return of a physiologic ECG signal as an indication of myocardial perfusion occurred. Note the contrast agent distribution in the LV and aorta versus the RV (**Figure 8, B and C**), providing evidence for systemic perfusion because it had been injected through the central venous line during cardiac arrest. RVEF and LVEF measured by CT volumetry were 16% (11%–21%) and 22% (20%–27%), respectively.

Discussion

This is the first study to show *in vivo* observations of a truly customized biventricular epicardial augmentation technology with regards to both anatomic and functional characteristics. The development of the biventricular epicardial augmentation system described here respects information and findings from excellent previous work on direct cardiac compression

Copyright © American Society of Artificial Internal Organs. Unauthorized reproduction of this article is prohibited.

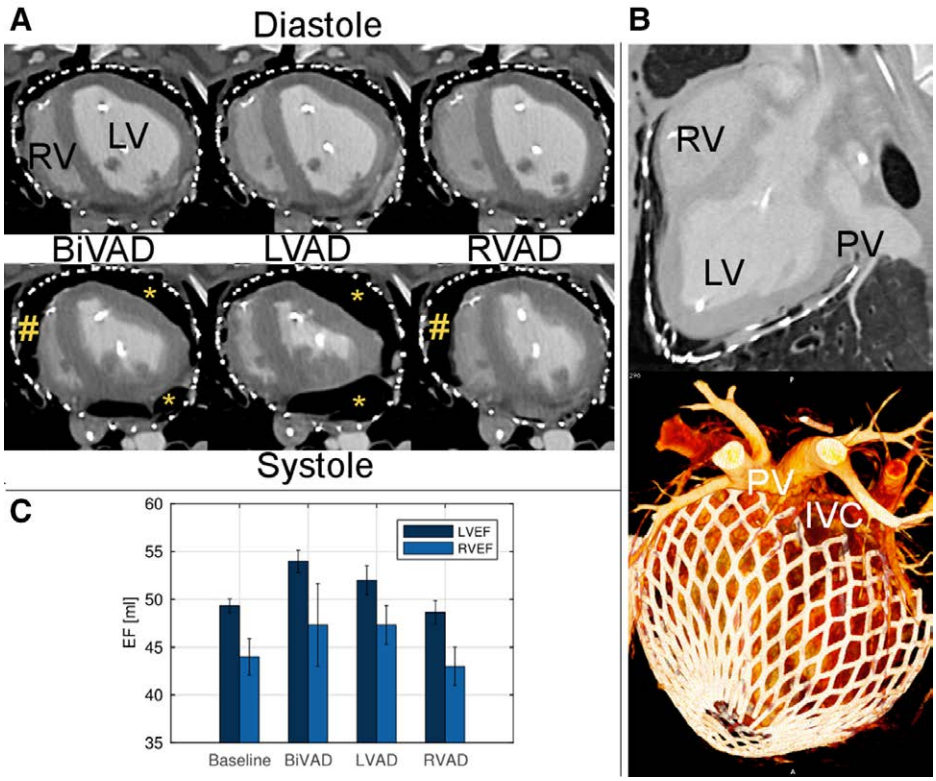

Figure 7. Postimplant computed tomography (CT) images. The effects of biventricular assist device (BiVAD), left ventricular (LV) assist device (LVAD) and right ventricular (RV) assist device (RVAD) support are shown in the end-diastolic and end-systolic phase. # indicates RV unit, * indicates LV units (**A**). In (**B**), the device fit is shown in sagittal view. A three-dimensional (3D) volume rendering shows the importance of the anatomic correct positioning of the device with regards to the major vessels. **C**: Ejection fraction (EF) from left and right ventricular CT volumetry. IVC, inferior vena cava; PV, pulmonary vein. full color online

devices. Our technology provides various novel solutions for the critical aspects, which in their combination results in excellent functionality of the system introduced here. This includes customized shape by segmentation of imaging data for optimal fit and exact positioning to address precise epicardial attachment and to avoid diastolic restriction. In addition, individually adjustable LV and RV support using three separate pneumatic units to provide biventricular support. Moreover, the development of an ECG-based control algorithm to account for synchronized mechanical support within each R- to T-wave interval allows to respect intra- and interindividual differences in systolic and diastolic duration in real time, and a self-expandable implant allows the reduction of procedural complexity and invasiveness, which may contribute to fast recovery and reduced complications.

The results show that the customized implants provided unconstrained cardiac function and no arrhythmias once they had been in place. This is an important observation as Mau *et al*. stated that "heart surrounding configuration … is likely to constrain ventricular filling and impair early diastolic relaxation."[7] In fact, our results showed a trend toward a decrease in time constants of the PV loops dp/dt_{min} and τ during mechanical support (see Figure, Supplemental Digital Content, http://links.lww.com/ASAIO/A186). Customization also enabled correct positioning of the implants in a minimally invasive procedure on the beating heart, ensuring correct positioning of the pneumatic units in their predefined locations. In this regard, we did not observe any signs of mitral regurgitation under epicardial augmentation in this model. However, in human HF patients with dilated ventricles, the device's mechanism of support may alter the state of already existing functional mitral valve regurgitation of varying degrees. Patient-specific design and positioning of the augmentation units using 3D imaging data analysis may be even useful in this context, particularly in case of posterior leaflet restriction. However, this remains to be studied.

Support pressures in the subsystemic range of 20–80 mm Hg gradually improved cardiac functional parameters in the acute failing heart model as indicated by increased SV and ESP, as well changes in RVEF and LVEF. This is comparable to what has been reported by other groups.[12] Importantly, this was only observed when ECG-based synchronization of support according to each cardiac cycle was optimized.

In contrast to current LVADs, this technology gradually increases SV and improves ventricular pressures without circumvention of the heart. For several reasons, this may be beneficial: it avoids blood contact, thereby, reducing the risk for complications, such as bleeding and stroke; applying direct pulsatile pressure to the dilated myocardial tissue reduces oxygen consumption and improves cardiac efficiency as recently shown in an ovine model of cardiomyoplasty.[13] Moreover, pulsatile support was shown to be superior to continuous flow with regard to myocardial recovery in humans.[14] The possibility to adjust the support to the amount that is individually required may be of interest in various ways: it opens room for novel individualized treatment and weaning protocols targeting the

Copyright © American Society of Artificial Internal Organs. Unauthorized reproduction of this article is prohibited.

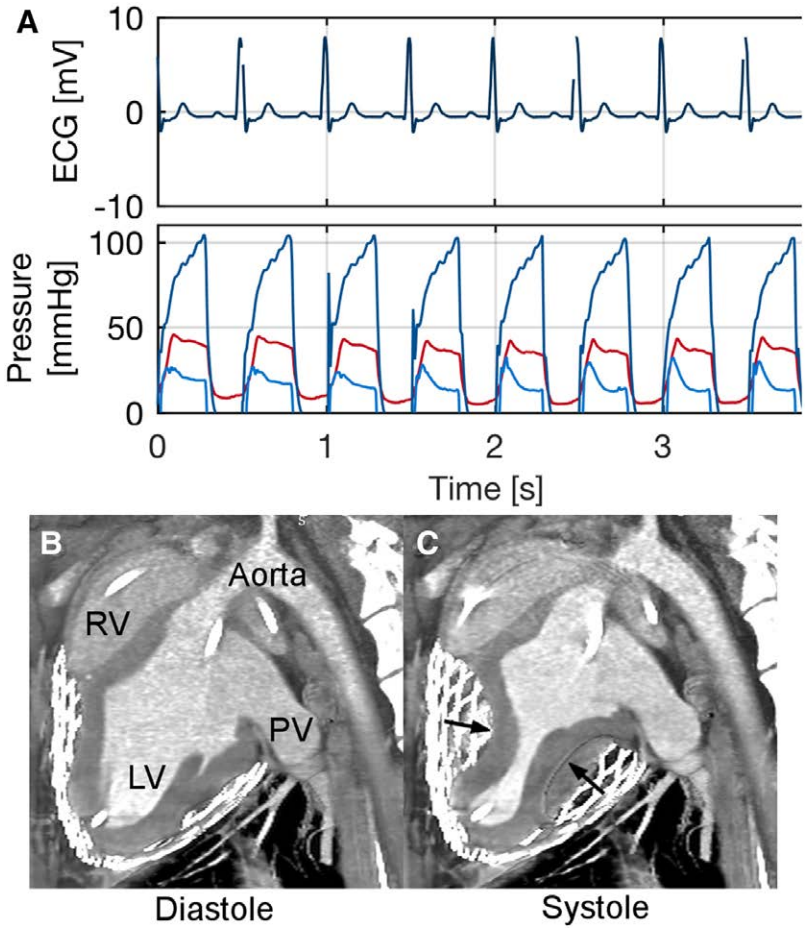

Figure 8. The functionality of the device demonstrated after cardiac arrest. The device is thereby triggered by an electrocardiogram (ECG) simulator. Left ventricular (LV) and support pressure curves (**A**), as well as end-diastolic and end-systolic computer tomography (CT) images with contrast agent distribution are shown (**B** and **C**). PV, pulmonary vein; RV, right ventricle; full color online

reverse remodeling potential of the heart. In addition, it shifts mechanical support to a nonobligatory device technology, which improves patient safety in situations of malfunction.

Another major observation in the current study is that the improvement of hemodynamic parameters is mediated only in the context of optimized synchronization of deflation to the isovolumetric relaxation phase. As shown, deflation of the pneumatic units immediately resulted in a ventricular pressure drop. During systole, this stopped the ejection of blood from the ventricles because the ventricular pressure had dropped below the augmented aortic/pulmonary arterial pressure. Statistical analysis of the data clearly indicated that with similar support pressures, shortened support duration leads to a reduction in LVSV and an increase in LVEDP when compared with optimal timing. Further prolongation of support may have an influence on diastolic filling over time, in particular in cases of higher HRs, and needs to be explored in more detail. This is an important finding not reported in this detail in the literature so far. It suggests that an adaptive, dynamic synchronization algorithm is mandatory for sustained epicardial mechanical support, particularly in the low-pressure range. It also indicates that improvement of ventricular function by epicardial augmentation is multifactorial, consisting of concise systolic inflation of augmentation units in predefined locations, timed diastolic deflation, and unrestricted diastolic filling. The latter may be of particular importance as McGarvey *et al*. observed velocity profiles that indicated the most notable effect on blood velocity was seen during diastolic deflation in pigs.[15]

In the current study, the device was used in both uni- and biventricular support modes. As shown, epicardial augmentation with subsystemic augmentation pressures in BiVAD mode and in LVAD mode increased EF from baseline in both ventricles (**Figure 7C**). Epicardial augmentation with 40 mm Hg of pressure in RVAD mode did not have significant effects on volumetric EF of both ventricles, but an increase in LVSV was observed. This biventricular effect may be explained by two geometrical effects of the support units during systolic inflation. First, direct effects on the myocardial region where pressure is applied, and second, a circumferential effect caused by the 3D changes during inflation of two or three support units. This observation is supported by Mau *et al*.,[7] who reported that cavity volume reduction was achieved because the septal–lateral short-axis change exceeded the anterior–posterior lengthening.

This is of particular importance because it is known that in patients with single LV failure, the right heart is deteriorating under mid-term to long-term support with current LVAD technology. Moreover, it is known that late-onset RV dysfunction is a complication of LVAD therapy, which has significant adverse implications with regard to patient outcome.[16] Although RV

Copyright © American Society of Artificial Internal Organs. Unauthorized reproduction of this article is prohibited.

function under epicardial support was already investigated in a previous study,[7] the long-term effects with regards to the functional state of the RV remain to be investigated.

Another important finding is the use of a fixed frequency support in situations of cardiac arrest over periods greater than 30 min. It allowed extended biventricular hemodynamic support and may be suitable for patients at risk. As shown in **Figure 8**, the functionality of this mode allows systemic perfusion with CO of around 2.5l·/min in this pig model. Even though resuscitation may not be the primary focus of this device, it clearly shows the effectiveness of this biventricular epicardial augmentation device regarding systemic perfusion. In the context of the development of clinical product for human use, its safety in terms of correct interpretation of the individual's ECG needs further exploration.

In conclusion, the present evaluation provides evidence that the use of a novel biventricular epicardial augmentation technology—by customized configuration and stable implant positioning, as well as synchronized timing of mechanical support according to each cardiac cycle—leads to improved hemodynamic parameters and might, thereby, beneficially modulate cardiac energy consumption. The fulfillment of these prerequisites was made possible by technical improvements in image processing, real-time signal analysis with modern electronic hardware, and algorithms.

The implantation and positioning on the beating heart appears safe and can be performed without sternotomy or the use of cardiopulmonary bypass. In addition, no anastomosis of foreign material to major blood vessels or the LV is necessary. This less-invasive procedure, thereby, reduces complexity and trauma to the patient, and its use may reduce complications associated with anticoagulation, including stroke and bleeding.

Finally, in the acute setting, we did not observe any deleterious injuries to the heart or large vessels during implantation and support. Based on our experience, the device is currently developed into a product system aiming at CE Mark and intended to be used in humans. There is a clear need for less invasive, biventricular devices that avoid blood contact for mechanical assistance of patients with advanced HF. With this device augmentation, pressures and volumes may be adjusted to meet the requirements of each individual patient. Thereby, it may be used earlier during the course of the disease process to bridge patients to transplantation. Because the technology avoids contact with the blood, it may reduce complications, including bleeding and stroke in patients at risk. One major aspect for long-term use of this technology in patients not having an option for transplantation is durability. This will be further optimized and tested, but clearly, one major goal is the development of a long-term device as an alternative to heart transplantation, which is limited by organ donor shortage.

Study Limitations

In this study, the drug-induced HF model used was only in part able to mimic the hemodynamic state of a failing heart. In addition, the geometry and mechanical structure of the hearts were normal. Even though we were able to test the device's functionality, this is clearly a limitation. The functionality of the implant is expected to be more efficient when used in hearts that underwent remodeling to a dilated, thin-walled morphology. It has been suggested previously that hemodynamic augmentation should be much more efficient during the latter condition.[17]

Acknowledgments

The authors thank Dr. Haug (Institute of Mathematical Statistics, Technical University of Munich, Germany) for advice concerning statistical analysis and interpretation of the data and Sabine Wuchenauer (Klinik für Diagnostische und Interventionelle Radiologie, Universitätsklinikum Ulm, Germany) for technical assistance during CT data acquisition and volumetric measurements.

References

1. Pruijsten RV, Lok SI, Kirkels HH, Klöpping C, Lahpor JR, de Jonge N: Functional and haemodynamic recovery after implantation of continuous-flow left ventricular assist devices in comparison with pulsatile left ventricular assist devices in patients with end-stage heart failure. *Eur J Heart Fail* 14: 319–325, 2012.
2. Miller LW, Guglin M, Rogers J: Cost of ventricular assist devices: can we afford the progress? *Circulation* 127: 743–748, 2013.
3. Kirklin JK, Naftel DC, Pagani FD, *et al*: Seventh INTERMACS annual report: 15,000 patients and counting. *J Heart Lung Transplant* 34: 1495–1504, 2015.
4. Benjamin EJ, Blaha MJ, Chiuve SE, *et al*: Heart Disease and Stroke Statistics-2017 Update: A report from the American Heart Association. *Circulation*. 131: e29–e322, 2017.
5. Roche ET, Horvath MA, Wamala I, *et al*: Soft robotic sleeve supports heart function. *Sci Transl Med*. 9: 1–12, 2017.
6. McConnell PI, Anstadt MP, Del Rio CL, Preston TJ, Ueyama Y, Youngblood BL: Cardiac function after acute support with direct mechanical ventricular actuation in chronic heart failure. *ASAIO J* 60: 701–706, 2014.
7. Mau J, Menzie S, Huang Y, Ward M, Hunyor S: Nonsurround, nonuniform, biventricular-capable direct cardiac compression provides Frank-Starling recruitment independent of left ventricular septal damage. *J Thorac Cardiovasc Surg* 142: 209–215, 2011.
8. Moreno MR, Biswas S, Harrison LD, *et al*: Assessment of minimally invasive device that provides simultaneous adjustable cardiac support and active synchronous assist in an acute heart failure model. *J Med Device*. 5: 41008, 2011.
9. Lowe JE, Hughes GC, Biswas SS: Non-blood-contacting biventricular support: Direct mechanical ventricular actuation. *Oper Tech Thorac Cardiovasc Surg*. 4: 345–351, 1999.
10. Bazett HC: An analysis of the time-relations of electrocardiograms. *Heart*. 7: 353–370, 1920.
11. Galecki A, Burzykowski T. Linear mixed-effects model, chapter 13 In Casella G, Fienberg S, Olkin I (eds). *Linear Mixed-Effects Models Using R*. Vol 102. New York: Springer Heidelberg Dordrecht London; 2013, pp. 245-273.
12. Artrip JH, Yi GH, Levin HR, Burkhoff D, Wang J: Physiological and hemodynamic evaluation of nonuniform direct cardiac compression. *Circulation* 100(19 suppl): II236–II243, 1999.
13. Kawaguchi O, Huang YF, Yuasa T, Shirota K, Carrington RA, Hunyor SN: Cardiomyoplasty reduces myocardial oxygen consumption: implications for direct mechanical compression. *Ann Thorac Surg* 74: 1092–1096; discussion 1096, 2002.
14. Kato TS, Chokshi A, Singh P, *et al*: Effects of continuous-flow versus pulsatile-flow left ventricular assist devices on myocardial unloading and remodeling. *Circ Heart Fail* 4: 546–553, 2011.
15. McGarvey JR, Kondo N, Takebe M, *et al*: Directed epicardial assistance in ischemic cardiomyopathy: flow and function using cardiac magnetic resonance imaging. *Ann Thorac Surg* 96: 577–585, 2013.
16. Kapelios CJ, Charitos C, Kaldara E, *et al*: Late-onset right ventricular dysfunction after mechanical support by a continuous-flow left ventricular assist device. *J Heart Lung Transplant* 34: 1604–1610, 2015.
17. Kawaguchi O, Goto Y, Futaki S, Ohgoshi Y, Yaku H, Suga H: The effects of dynamic cardiac compression on ventricular mechanics and energetics. Role of ventricular size and contractility. *J Thorac Cardiovasc Surg* 107: 850–859, 1994.

Copyright © American Society of Artificial Internal Organs. Unauthorized reproduction of this article is prohibited.